ESAIM: M2AN 51 (2017) 1805–1826
DOI: 10.1051/m2an/2016079

ESAIM: Mathematical Modelling and Numerical Analysis
www.esaim-m2an.org

ASYMPTOTIC-PRESERVING WELL-BALANCED SCHEME FOR THE ELECTRONIC M_1 MODEL IN THE DIFFUSIVE LIMIT: PARTICULAR CASES

Sébastien Guisset[1,2], Stéphane Brull[1], Emmanuel D'Humières[2] and Bruno Dubroca[2]

Abstract. This work is devoted to the derivation of an asymptotic-preserving scheme for the electronic M_1 model in the diffusive regime. The case without electric field and the homogeneous case are studied. The derivation of the scheme is based on an approximate Riemann solver where the intermediate states are chosen consistent with the integral form of the approximate Riemann solver. This choice can be modified to enable the derivation of a numerical scheme which also satisfies the admissible conditions and is well-suited for capturing steady states. Moreover, it enjoys asymptotic-preserving properties and handles the diffusive limit recovering the correct diffusion equation. Numerical tests cases are presented, in each case, the asymptotic-preserving scheme is compared to the classical HLL [A. Harten, P.D. Lax and B. Van Leer, *SIAM Rev.* **25** (1983) 35–61.] scheme usually used for the electronic M_1 model. It is shown that the new scheme gives comparable results with respect to the HLL scheme in the classical regime. On the contrary, in the diffusive regime, the asymptotic-preserving scheme coincides with the expected diffusion equation, while the HLL scheme suffers from a severe lack of accuracy because of its unphysical numerical viscosity.

Mathematics Subject Classification. 65C20, 65M12.

Received April 22, 2015. Revised September 1, 2016. Accepted December 9, 2016.

1. Introduction

In inertial confinement fusion, nanosecond laser pulses are used to ignite a deuterium-tritium target. An accurate description of this process is necessary for the understanding of laser-matter interactions and for target design. Numerous physical phenomena such as, parametric [36, 67] and hydrodynamic [32, 74, 81] instabilities, laser-plasma absorption [73], wave damping [57], energy redistribution [70] inside the plasma and hot spots formation [12, 65] from which the thermonuclear reactions propagate depend on the electron heat transport. The most popular electron heat transport theory was developed by Spitzer and Härm [76] who first solved the electron kinetic equation by using the expansion of the electron mean free path to the temperature scale length (denoted ε in this paper). Considering the distribution function of particles close to equilibrium, its deviation

Keywords and phrases. Electronic M_1 moment model, approximate Riemann solvers, Godunov type schemes, asymptotic preserving schemes, diffusive limit, plasma physics.

[1] Université Bordeaux, IMB, UMR 5251, 33405 Talence, France. guisset@celia.u-bordeaux1.fr

[2] Université Bordeaux, CELIA, UMR 5107, 33400 Talence, France.

from the Maxwellian distribution function can be computed and the electron transport coefficients in a fully ionised plasma without magnetic field are derived. However, even if the electron heat transport is essential, it is not correctly described in large inertial confinement fusion tools. Indeed, when the electron mean free path exceeds about 2×10^{-3} times the temperature gradient length, the local electron transport model of Spitzer and Härm fails. The transport coefficients were derived in the case where the isotropic part of the electron distribution function remains close to the Maxwellian function. The results of Spitzer and Härm have been reproduced in several approaches [4,11,75] which develop another technique of solution to the integral equation for the electron distribution function introduced many years ago by Chapman and Enskog [23] for neutral gases. Therefore, kinetic approaches seem necessary in the context of inertial confinement fusion. In such multiscale issues, kinetic solvers are often very computationally expensive and usually limited to time and length much shorter than those studied with hydrodynamic simulations. It is then a challenge to describe kinetic effects using a reduced kinetic code on fluid time scales.

It is considered that angular moments models provide higher accuracy than fluid model because the velocity modulus (denoted ζ in this work) is kept as a variable. The integration of the kinetic equation to obtain such models is performed only in angle (integration on the unit sphere). Angular moments represent angular average quantities of the distribution function. Therefore, they can be seen as intermediate models between kinetic and classic fluid models. Originally, the moment closure hierarchy introduced by Grad [40] leads to a hyperbolic set of equations for flows close to equilibrium but may suffer from closure breakdown and lead to unrealisable macroscopic moments. Grad hierarchy is derived from a truncated polynomial series expansion for the velocity distribution function near the Maxwellian equilibrium and does not ensure the positivity of the distribution function. Other moment closure approaches have been investigated based on entropy minimisation principles [2, 61, 68, 69, 77]. The distribution function derived, verifies a minimum entropy property and the consistency with the set of moments. Fundamental mathematical properties [42,66] such as positivity of the distribution function, hyperbolicity and entropy dissipation can be exhibited. Levermore [61] proposed a hierarchy of minimum-entropy closure where the lowest order closure are the Maxwellian and Gaussian closure. In the present case, the aim is different. Here the energy of particles constitutes a free parameter. Then we integrate only the kinetic equation with respect to the angle variable and we return only the energy of particles as kinetic variable. By using a closure defined from a minimisation entropy principle, we obtain the M_1 model [33, 34, 63]. The M_1 model is largely used in various applications such as radiative transfer [7,24,35,71,72,79,80] or electronic transport [33, 63]. The M_1 model is known to satisfy fundamental properties such as the positivity of the first angular moment, the flux limitation and conservation of total energy. Also, it correctly recovers the asymptotic diffusion equation in the limit of long time behaviour with important collisions [34].

One challenging issue is to derive numerical schemes satisfying fundamental properties. For example, the classical HLL scheme [44] ensures the positivity of the first angular moment and the flux limitation property. However, this scheme fails in recovering the correct limit diffusion equation in the asymptotic regime [3]. Therefore, numerous numerical schemes have been derived over the last 20 years to recover the correct asymptotic limit. These schemes are able to handle multiscales situations and are called asymptotic-preserving (AP) scheme. They are consistent with the macroscopic model when ε tends to zero and are uniformly stable with respect to ε. AP schemes also avoid the coupling of multiscales equations where the coupling conditions at the interface can be difficult to obtain. Early works on AP schemes have been performed in [46–49, 58, 59]. These works have been largely extended in the frame of kinetic equations in fluid and diffusive regimes [17, 25, 50, 54]. The time stiffness induced by the collisional operator led to propose a decomposition of the distribution function between an equilibrium and a deviation [5, 14, 19, 45, 51, 53, 55, 60]. In [13], a two steps method based on a relaxation scheme and a well-balanced scheme step is proposed, (see [9, 52] for more details on the relaxation scheme framework). The derivation of well-balanced schemes also helps to design AP schemes [38,39] (see also [1, 9, 10, 18, 21, 22, 37, 41] for details on well-balanced schemes in different frameworks). The AP frame was also largely extended to the quasi-neutral limit [26–30, 43]. In [7], an $HLLC$ scheme is proposed to solve the M_1 model of radiative transfer in two space dimensions. The $HLLC$ approximate Riemann solver considered and relevant numerical approximations of extreme wavespeeds give the asymptotic-preserving property. Similar ideas were also developed in [6], where a relaxation scheme is exhibited. In order to derive suitable schemes pertinent for transport and diffusion regimes, different authors proposed modified Godunov-type schemes in order to include sources terms [41]. The numerical viscosity is modified in [15,16,38,39] to correctly recover the expected diffusion regimes but extensions seem challenging issues. In [8], the approximate HLL Riemann solver is modified to include a collisional source term. The resulting numerical scheme satisfies all the fundamental properties and a clever correction enables to recover the good diffusion equation in the asymptotic limit.

In this paper, we consider the M_1 model for the electronic transport [33,63,64] in a Lorentzian plasma where ions are supposed fixed. The moment system studied writes

$$\begin{cases} \partial_t f_0(t,x,\zeta) + \zeta\partial_x f_1(t,x,\zeta) + E(x)\partial_\zeta f_1(t,x,\zeta) = 0, \\ \partial_t f_1(t,x,\zeta) + \zeta\partial_x f_2(t,x,\zeta) + E(x)\partial_\zeta f_2(t,x,\zeta) - \dfrac{E(x)}{\zeta}(f_0(t,x,\zeta) - f_2(t,x,\zeta)) \\ \qquad\qquad = -\dfrac{2\alpha_{ei}(x) f_1(t,x,\zeta)}{\zeta^3}, \end{cases} \tag{1.1}$$

where f_0, f_1 and f_2 are the first three angular moments of the electron distribution function f. Omitting the x and t dependency, they are given by

$$f_0(\zeta) = \zeta^2 \int_{-1}^{1} f(\mu,\zeta)\mathrm{d}\mu, \;\; f_1(\zeta) = \zeta^2 \int_{-1}^{1} f(\mu,\zeta)\mu\mathrm{d}\mu, \;\; f_2(\zeta) = \zeta^2 \int_{-1}^{-1} f(\mu,\zeta)\mu^2\mathrm{d}\mu. \tag{1.2}$$

The coefficient α_{ei} is a positive physical function which may depend on x, E represents the electrostatic field and ζ the velocity modulus. In the present study the electric field is considered constant. The fundamental point of the moments models is the definition of the closure which writes the highest moment as a function of the lower ones. This closure relation corresponds to an approximation of the underlying distribution function, which the moments system is constructed from. In the M_1 problem we need to define f_2 as a function of f_0 and f_1. The closure relation originates from an entropy minimisation principle [61,68]. The moment f_2 can be calculated [33,35] as a function of f_0 and f_1

$$f_2(t,x,\zeta) = \chi\left(\frac{f_1(t,x,\zeta)}{f_0(t,x,\zeta)}\right) f_0(t,x,\zeta), \qquad \text{with} \qquad \chi(\alpha) \approx \frac{1+\alpha^2+\alpha^4}{3}\cdot \tag{1.3}$$

The closure relation in equation (1.3) is not the exact M_1 closure but an approximation. Therefore it is not clear the model inherit hyperbolicity and entropy decay. This approximation is used since one can not find an exact expression for the highest order moment as a function of lower ones. The set of admissible states [33] is defined by

$$\mathcal{A} = \Big((f_0, f_1) \in \mathbb{R}^2, \;\; f_0 \geq 0, \quad |f_1| \leq f_0\Big). \tag{1.4}$$

A challenging issue is to derive a numerical scheme for the electron M_1 model (1.1) satisfying all the fundamental properties and which handles correctly the diffusive limit recovering the good diffusion equation. Such a scheme could then have a direct access to all the nonlocal regimes and their related physical effects described above while the other numerical schemes breakdown in such regimes. Different complications arise when considering such an issue. Firstly, the electronic M_1 model (1.1) is nonlinear. Because, of the entropic closure, the angular moment f_2 is a nonlinear function of f_0 and f_1. Secondly, the approach undertaken must be sufficiently general to correctly take into account the source term $-E(f_0(t,x,\zeta) - f_2(t,x,\zeta))/\zeta$. One must notice, that this term is closely related to the term $E\partial_\zeta f_2(t,x,\zeta)$, it plays an important role for low energies and can not be treated as a collisional source term. Thirdly, for the purpose of realistic physical applications, one may require to correctly capture steady states. In the case of near-equilibrium configurations such a well-balancing property is then desired. Also, the physical parameter α_{ei} is a function of x and cannot be treated as a constant. Finally, the space and energy dependencies of the angular moments, lead to a very complex diffusion equation in the asymptotic limit with mixed derivatives.

In this paper, the case without electric field and the homogeneous case are studied. The extension to the general case is beyond the scope of this paper. However, the generalisation to the general problem requires a deep understanding of the two configurations studied here. The approach retained is noticeably different with [6,7,44]. The derivation of the scheme is based on an approximate Riemann solver where the intermediate states are chosen consistent with the integral form of the approximate Riemann solver. This choice can be modified to enable the derivation of a scheme which also satisfies the admissibility conditions (1.4) and is well-suited for capturing steady states. Moreover, it enjoys asymptotic-preserving properties and correctly handles the diffusive limit recovering the good diffusion equation.

We first introduce the model without electrostatic field and its diffusive limit in Section 2. The limits of the classical HLL scheme [44] are briefly recalled before introducing the derivation of the new numerical scheme. The asymptotic-preserving property is exhibited. Then, Section 3 is devoted to the homogeneous case with an electric field. We point out the great difficulties encountered when using a relaxation approach in order to include the source term $-E(x)(f_0(t,x,\zeta) - f_2(t,x,\zeta))/\zeta$. Then, the derivation of an asymptotic-preserving scheme following the method introduced in the previous section is detailed and the well-balanced and asymptotic-preserving properties are analysed. In Section 4, different numerical tests are presented to highlight the efficiency of the present method. We conclude the paper in Section 5.

2. Case without electrostatic field

The first simplified case we consider is given by system (1.1) without electrostatic field E. In this case the M_1 model (1.1) writes

$$\begin{cases} \partial_t f_0 + \zeta \partial_x f_1 = 0, \\ \partial_t f_1 + \zeta \partial_x f_2 = -\dfrac{2\alpha_{ei}}{\zeta^3} f_1. \end{cases} \tag{2.1}$$

A very similar system was considered in [6] in the frame of radiative transfer and a relaxation scheme was proposed. The same procedure could be applied in this case, however we introduce a different approach based on approximate Riemann solvers.

2.1. Model and diffusive limit

We consider the following diffusion scaling

$$\tilde{t} = t/t^*, \quad \tilde{x} = x/x^*, \quad \tilde{\zeta} = \zeta/v_{th}, \quad \tilde{E} = Ex^*/v_{th}.$$

The parameters t^* and x^* are chosen such that $\tau_{ei}/t^* = \varepsilon^2$, $\lambda_{ei}/x^* = \varepsilon$, where τ_{ei} is the electron-ion collisional period, λ_{ei} the electron-ion mean free path and v_{th} the thermal velocity defined by $v_{th} = \lambda_{ei}/\tau_{ei}$. The positive parameter ε is devoted to tend to zero. In that case, omitting the tilde notation, system (2.1) rewrites

$$\begin{cases} \varepsilon \partial_t f_0^\varepsilon + \zeta \partial_x f_1^\varepsilon = 0, \\ \varepsilon \partial_t f_1^\varepsilon + \zeta \partial_x f_2^\varepsilon = -\dfrac{2\sigma}{\zeta^3} \dfrac{f_1^\varepsilon}{\varepsilon}, \end{cases} \tag{2.2}$$

where the coefficient σ represents a positive function of x defined as

$$\sigma(x) = \frac{\tau_{ei}\alpha_{ei}(x)}{v_{th}^3}\cdot$$

Inserting the following Hilbert expansion of f_0^ε and f_1^ε

$$\begin{cases} f_0^\varepsilon = f_0^0 + \varepsilon f_0^1 + O(\varepsilon^2), \\ f_1^\varepsilon = f_1^0 + \varepsilon f_1^1 + O(\varepsilon^2), \end{cases} \tag{2.3}$$

into the second equation of (2.2) leads to

$$f_1^0 = 0. \tag{2.4}$$

Using the definition (1.3), it follows that

$$f_2^0 = f_0^0/3.$$

So, the second equation of (2.2) gives

$$f_1^1 = -\frac{\zeta^4}{6\sigma}\partial_x f_0^0. \tag{2.5}$$

Using the previous equation and the first equation of (2.2) finally leads to the diffusion equation for f_0^0

$$\partial_t f_0^0(t,x) - \partial_x\left(\frac{\zeta^5}{6\sigma(x)}\partial_x f_0^0(t,x)\right) = 0. \tag{2.6}$$

Here we have omitted the tilde notation, writing this diffusion equation in non-rescaled (dimensional) variables we obtain

$$\partial_t f_0^0(t,x) - \partial_x\left(\frac{\zeta^5}{6\alpha_{ei}(x)}\partial_x f_0^0(t,x)\right) = 0. \tag{2.7}$$

2.2. The numerical method

In this part, we first study the limit of the HLL scheme in the diffusive regime. Then a Godunov-type scheme based on an approximate Riemann solver is proposed.

2.2.1. Limit of the HLL scheme

Introduce a uniform mesh with constant space step $\Delta x = x_{i+1/2} - x_{i-1/2}$, $i \in Z$ and a time step Δt. We consider a piecewise constant approximate solution $U^h(x,t^n) \in \mathbb{R}^2$ at time t^n

$$U^h(x,t^n) = U_i^n \quad if \quad x \in [x_{i-1/2}, x_{i+1/2}]$$

with $U_i^n = {}^t(f_{0i}^n, f_{1i}^n)$. The classical HLL scheme [44] for the system (2.6), in the case where the minimum and maximum velocity waves involved in the approximate Riemann solver are chosen equal to $-\zeta$ and ζ, writes

$$\begin{cases} \varepsilon\dfrac{f_{0i}^{n+1,\varepsilon} - f_{0i}^{n,\varepsilon}}{\Delta t} + \zeta\dfrac{f_{1i+1}^{n,\varepsilon} - f_{1i-1}^{n,\varepsilon}}{2\Delta x} - \zeta\Delta x\dfrac{f_{0i+1}^{n,\varepsilon} - 2f_{0i}^{n,\varepsilon} + f_{0i-1}^{n,\varepsilon}}{2\Delta x^2} = 0, \\ \varepsilon\dfrac{f_{1i}^{n+1,\varepsilon} - f_{1i}^{n,\varepsilon}}{\Delta t} + \zeta\dfrac{f_{2i+1}^{n,\varepsilon} - f_{2i-1}^{n,\varepsilon}}{2\Delta x} - \zeta\Delta x\dfrac{f_{1i+1}^{n,\varepsilon} - 2f_{1i}^{n,\varepsilon} + f_{1i-1}^{n,\varepsilon}}{2\Delta x^2} = -\dfrac{2\sigma_i}{\zeta^3}\dfrac{f_{1i}^{n+1,\varepsilon}}{\varepsilon}. \end{cases} \tag{2.8}$$

We introduce the discrete Hilbert expansions

$$\begin{cases} f_{0i}^{\varepsilon} = f_{0i}^{n,0} + \varepsilon f_{0i}^{n,1} + O(\varepsilon^2), \\ f_{1i}^{n,\varepsilon} = f_{1i}^{n,0} + \varepsilon f_{1i}^{n,1} + O(\varepsilon^2). \end{cases} \tag{2.9}$$

At the order ε^{-1}, the second equation of (2.8) gives

$$f_{1i}^{n,0} = 0$$

and using the definition (1.3), it follows that

$$f_{2i}^{n,0} = f_{0i}^{n,0}/3.$$

At the order ε^0, the second equation of (2.8) gives

$$f_{1i}^{n,1} = -\frac{\zeta^3}{3\sigma_i}\frac{f_{0i+1}^{n,0} - f_{0i-1}^{n,0}}{2\Delta x}.$$

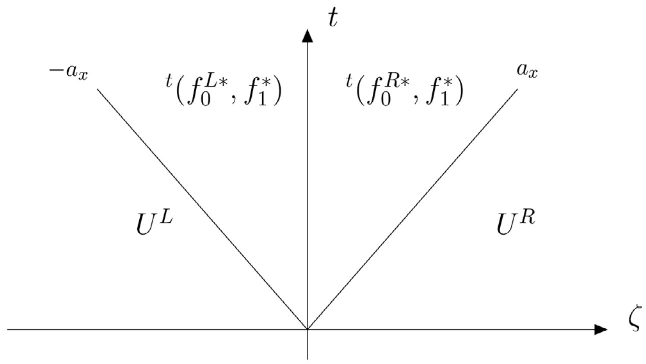

FIGURE 1. Structure solution of the approximate Riemann problem.

However, because of the diffusive part of the HLL scheme, the first equation of (2.8) also leads to

$$\frac{f_{0i+1}^{n,0} - 2f_{0i}^{n,0} + f_{0i-1}^{n,0}}{\Delta x^2} = 0$$

which is not the diffusion equation expected for f_0^0. The diffusive part of the HLL scheme gives an unphysical numerical viscosity and leads to the wrong asymptotic behaviour.

2.2.2. Derivation of the scheme

The numerical scheme considered in the previous part to compute f_{1i}^{n+1} at each time step is conserved and writes

$$\frac{f_{1i}^{n+1} - f_{1i}^n}{\Delta t} + \zeta \frac{f_{2i+1}^n - f_{2i-1}^n}{2\Delta x} - a_x \frac{f_{1i+1}^n - 2f_{1i}^n + f_{1i-1}^n}{2\Delta x} = -\frac{2\sigma_i}{\zeta^3} f_{1i}^{n+1}. \tag{2.10}$$

However, in order to determine f_{0i}^{n+1} at each time step, a Godunov-type scheme based on an approximate Riemann solver is considered. The ideas introduced in [6, 8, 9, 41] in order to include the contribution of source terms, urge to consider approximate Riemann solvers which own a stationary discontinuity (0-contact discontinuity). Therefore, we introduce the following approximate Riemann solvers at each cell interface, denoted by $U_{\mathcal{R}}(x/t, U^L, U^R)$, defined by

$$U_{\mathcal{R}}(x/t, U^L, U^R) = \begin{cases} U^L & \text{if} \quad x/t < -a_x, \\ U^{L*} & \text{if} \quad -a_x < x/t < 0, \\ U^{R*} & \text{if} \quad 0 < x/t < a_x, \\ U^R & \text{if} \quad a_x < x/t, \end{cases} \tag{2.11}$$

where $U^{L*} = {}^t(f_0^{L*}, f_1^*)$, $U^{R*} = {}^t(f_0^{R*}, f_1^*)$ and the minimum and maximum velocity waves $-a_x$ and a_x. Note, we choose the two velocity waves to be opposite. The structure solution of the approximate Riemann problem is displayed in Figure 1. At the interface $x_{i+\frac{1}{2}}$, the quantities U^L and U^R stand for $U_i = {}^t(f_{0i}, f_{1i})$ and $U_{i+1} = {}^t(f_{0i+1}, f_{1i+1})$. Contrarily to the classical HLL scheme [78] two intermediate states U^{L*} and U^{R*} are introduced. The second components of the two intermediate states are chosen equal, ie $f_1^{L*} = f_1^{R*} = f_1^*$. It will be shown that in spite of this simplification in the approximate Riemann solver an asymptotic-preserving scheme can be derived.

The approximate solution at time $t^n + \Delta t$ is chosen as

$$U^h(x, t^n + \Delta t) = U_{\mathcal{R}}\left(\frac{x - x_{i+1/2}}{t^n + \Delta t}, U_i, U_{i+1}\right) \qquad \text{if} \qquad x \in [x_i, x_{i+1}]. \tag{2.12}$$

As the following CFL condition is respected

$$\Delta t \leq \frac{\Delta x}{2a_x},$$

the piecewise constant approximate solution is then obtained

$$U_i^{n+1} = \frac{1}{\Delta x}\int_{x_{i-1/2}}^{x_{i+1/2}} U^h(x, t^{n+1})\mathrm{d}x. \tag{2.13}$$

The intermediate states f_0^{L*}, f_0^{R*} and f_1^* must be defined. Integrating the first equation of (2.1) on $[-a_x\Delta t, a_x\Delta t]\times[0,\Delta t]$ and multiplying by $\frac{1}{2a_x\Delta t}$, gives the following consistency condition

$$\frac{f_0^{L*}+f_0^{R*}}{2} = \frac{f_0^L+f_0^R}{2} - \frac{1}{2a_x}\left(\zeta f_1^R - \zeta f_1^L\right). \tag{2.14}$$

The unknowns f_0^{L*} and f_0^{R*} will be chosen in order to satisfy this consistency condition (2.14). The same procedure using the second equation of (2.1) gives

$$f_1^* = \frac{f_1^L+f_1^R}{2} - \frac{1}{2a_x}\left(\zeta f_2^R - \zeta f_2^L\right) - \frac{2}{\zeta^3}\frac{1}{2a_x\Delta t}\int_{-a_x\Delta t}^{a_x\Delta t}\int_0^{\Delta t}\alpha_{ei}(x)f_1(x,t)\mathrm{d}t\mathrm{d}x. \tag{2.15}$$

The following approximation is made

$$\frac{1}{2a_x\Delta t}\int_{-a_x\Delta t}^{a_x\Delta t}\int_0^{\Delta t}\alpha_{ei}(x)f_1(x,t)\mathrm{d}t\mathrm{d}x = \bar{\alpha}_{ei}\Delta t f_1^*, \tag{2.16}$$

with $\bar{\alpha}_{ei} = \alpha(0)$. In the approximation (2.16), the solution is chosen at time Δt. Indeed, since the source term becomes stiff in the limit regime an implicit treatment is considered. Using (2.16) in (2.15), it follows that

$$f_1^* = \frac{\zeta^3}{\zeta^3+2\bar{\alpha}_{ei}\Delta t}\left[\frac{f_1^L+f_1^R}{2} - \frac{1}{2a_x}(\zeta f_2^R - \zeta f_2^L)\right]. \tag{2.17}$$

Finally the following definition of f_1^* is chosen

$$f_1^* = \frac{2a_x\zeta^3}{2a_x\zeta^3+2\bar{\alpha}_{ei}\Delta x}\left[\frac{f_1^L+f_1^R}{2} - \frac{1}{2a_x}\left(\zeta f_2^R - \zeta f_2^L\right)\right]. \tag{2.18}$$

It will be shown in the next part, that this choice of intermediate state enables to obtain the good asymptotic-preserving property. Also, this definition recovers the formalism introduced in [7,8].

If the intermediate states f_0^{L*} and f_0^{R*} are chosen such that $f_0^{L*} = f_0^{R*} = \tilde{f}_0$, the consistency relation (2.14) is satisfied but one recovers the usual HLL scheme which does not behave correctly in the limit. Therefore the following definitions are proposed

$$\begin{cases} f_0^{L*} = \tilde{f}_0 - \Gamma, \\ f_0^{R*} = \tilde{f}_0 + \Gamma, \end{cases} \tag{2.19}$$

with

$$\tilde{f}_0 = \frac{f_0^L+f_0^R}{2} - \frac{1}{2a_x}(\zeta f_1^R - \zeta f_1^L), \tag{2.20}$$

and Γ is a coefficient which needs to be fixed. Obviously, the definitions (2.19) respect the consistency relation (2.14). The coefficient Γ is now fixed by considering the Rankine−Hugoniot relations

$$\begin{cases} f_0^{L*} = f_0^L - \dfrac{\zeta}{a_x}(f_1^* - f_1^L), \\ f_0^{R*} = f_0^R - \dfrac{\zeta}{a_x}(f_1^R - f_1^*). \end{cases} \tag{2.21}$$

By injecting (2.21) into (2.19), it follows that

$$\Gamma = \frac{1}{2}\left[f_0^R - f_0^L - \frac{\zeta}{a_x}(f_1^L - 2f_1^* + f_1^R)\right]. \tag{2.22}$$

Unfortunately, the intermediate states defined here are not always admissible. In order to enforce the admissibility conditions (1.4) of the numerical solution, we propose to modify the states f_0^{L*} and f_0^{R*} such that

$$\begin{cases} f_0^{L*} = \tilde{f}_0 - \Gamma\theta, \\ f_0^{R*} = \tilde{f}_0 + \Gamma\theta, \end{cases} \tag{2.23}$$

where $\theta \in [0, 1]$ is fixed to ensure the admissibility conditions.

Remark 2.1. In the case $\theta = 0$, the admissibility requirements (1.4) are fulfilled.

Indeed, in this case system (2.23) gives $f_0^{R*} = f_0^{L*} = \tilde{f}_0$ and f_1^* is given by (2.18). Since $2a_x\zeta^3/(2a_x\zeta^3+\sigma\Delta x) \leq 1$ it follows that $f_1^* \leq f_0^{R*} = f_0^{L*}$. Then the parameter θ is computed as the largest possible such that

$$\begin{cases} f_0^{R*} - |f_1^*| \geq 0, \\ f_0^{L*} - |f_1^*| \geq 0, \\ f_0^{R*} \geq 0 \ \text{ and } \ f_0^{L*} \geq 0. \end{cases} \tag{2.24}$$

Equations (2.22)–(2.24) lead to the following condition

$$\tilde{\theta} = \frac{\tilde{f}_0 - |f_1^*|}{|\Gamma|} \geq 0. \tag{2.25}$$

Finally, θ is chosen as $\theta = \min(\tilde{\theta}, 1)$. In the case where the parameter θ is not equal to 1, one observes that the Rankine−Hugoniot conditions (2.21) are not respected. However, the admissibility of the numerical solution is privileged here. In addition, despite the loss of the Rankine−Hugoniot conditions (2.21), the consistency of the approximate Riemann solver with the integral form of (2.1) ensures the efficiency of the method [44]. This is also observed in practice when considering the different numerical test cases.

The unknown f_{0i}^{n+1} is finally computed using (2.13)

$$f_{0i}^{n+1} = \frac{a_x\Delta t}{\Delta x} f_{0i-1/2}^{R*} + \left(1 - \frac{2a_x\Delta t}{\Delta x}\right) f_{0i}^n + \frac{a_x\Delta t}{\Delta x} f_{0i+1/2}^{L*}, \tag{2.26}$$

with the relations (2.23).

The wavespeed a_x is fixed using the ideas introduced in [6]. It is known that the electronic M_1 model without electric field is hyperbolic symmetrizable [61] and the eigenvalues of the Jacobian matrix always belong in the interval $[-\zeta, \zeta]$. Therefore, we set $a_x = \zeta$.

2.3. Admissibility and asymptotic-preserving properties

In this part the admissibility of the numerical solution and the asymptotic-preserving property of the scheme (2.10)−(2.18)−(2.23)−(2.26) are proved. It is shown that when ε tends to zero, the scheme is consistent with the limit diffusion equation (2.6).

Proposition 2.2. *The numerical scheme* (2.10)−(2.18)−(2.23)−(2.26) *preserves the admissibility of the numerical solutions.*

Proof. We remark that equation (2.35) rewrites

$$f_{1i}^{n+1} = \alpha \frac{a_x \Delta t}{\Delta x} \tilde{f}_{1i-1/2} + \alpha \left(1 - \frac{2a_x \Delta t}{\Delta x}\right) f_{1i}^n + \alpha \frac{a_x \Delta t}{\Delta x} \tilde{f}_{1i+1/2}, \tag{2.27}$$

with $\alpha = \zeta^3/(\zeta^3 + 2\alpha_{ei}\Delta t) \in [0,1]$ and

$$\tilde{f}_{1i+1/2} = \frac{f_{1i}^n + f_{1i+1}^n}{2} - \frac{1}{2a_x}(\zeta f_{2i+1}^n - \zeta f_{2i}^n).$$

Using equation of (2.26) and (2.27) a direct calculation of $f_{0i}^{n+1} \pm f_{1i}^{n+1}$ shows that the condition (2.25) ensure the admissibility of the numerical solution. Also, it can be seen geometrically since the admissible set a convex cone and α belongs to $[0,1]$. □

Theorem 2.3 (Consistency in the limit regime)**.** *When ε tends to zero, the unknown $f_{0i}^{n+1,0}$ given by the numerical scheme (2.10)–(2.18)–(2.23)–(2.26) satisfies the following discrete equation*

$$\frac{f_{0i}^{n+1,0} - f_{0i}^{n,0}}{\Delta t} - \frac{\zeta}{\Delta x}\left[\frac{\zeta^3}{6\bar{\sigma}_{i+1/2}\Delta x}\left[(\zeta f_{0i+1}^{n,0} - \zeta f_{0i}^{n,0})\right] - \frac{\zeta^3}{6\bar{\sigma}_{i-1/2}\Delta x}\left[(\zeta f_{0i}^{n,0} - \zeta f_{0i-1}^{n,0})\right]\right] = 0. \tag{2.28}$$

Proof. Following the same approach as in [7,8], using the diffusive scaling and equation (2.26) leads to

$$\varepsilon \frac{f_{0i}^{n+1} - f_{0i}^n}{\Delta t} = \frac{a_x}{\Delta x} f_{0i+1/2}^{L*} - \frac{2a_x}{\Delta x} f_{0i}^n + \frac{a_x}{\Delta x} f_{0i-1/2}^{R*}, \tag{2.29}$$

where the intermediate states f_0^{L*} and f_0^{R*} are given by (2.23) and (2.18) rewrites

$$f_1^* = \frac{2a_x\zeta^3}{2a_x\zeta^3 + 2\bar{\sigma}\Delta x/\varepsilon}\left[\frac{f_1^L + f_1^R}{2} - \frac{1}{2a_x}(\zeta f_2^R - \zeta f_2^L)\right]. \tag{2.30}$$

As soon as ε tends to zero, we obtain $f_1^* = 0$. We now suppose that $f_{1i}^n = 0$ in the limit ε tends to zero. In this case, the definition (2.25) leads to

$$\tilde{\theta} = \frac{f_0^L + f_0^R}{|f_0^L - f_0^R|} \geq 1.$$

Then the parameter θ is equal to 1.

Remark 2.4. In the diffusive regime when ε tends to zero, no limitation on the intermediates states (2.23) is required.

Using the definition (2.23), it follows that the intermediate states f_0^{L*} and f_0^{R*} are given by

$$\begin{cases} f_0^{L*} = f_0^L - \dfrac{\zeta}{a_x}(f_1^* - f_1^L), \\ f_0^{R*} = f_0^R - \dfrac{\zeta}{a_x}(f_1^R - f_1^*). \end{cases} \tag{2.31}$$

The discrete Hilbert expansions (2.9) are now used. Inserting the previous expressions in equation (2.29), considered at the order ε^0, gives no information since the terms cancel each other out. However, at the order ε^1, the expressions (2.31), (2.30) and equation (2.29) lead to

$$\begin{cases} f_0^{L*,1} = f_0^{L,1} - \dfrac{\zeta}{a_x}(f_1^{*,1} - f_1^{L,1}), \\ f_0^{R*,1} = f_0^{R,1} - \dfrac{\zeta}{a_x}(f_1^{R,1} - f_1^{*,1}), \end{cases} \tag{2.32}$$

with

$$f_1^{*,1} = -\frac{\zeta^3}{6\bar{\sigma}\Delta x}\left(\zeta f_0^{R,n,0} - \zeta f_0^{L,n,0}\right) \tag{2.33}$$

and

$$\frac{f_{0i}^{n+1,0} - f_{0i}^{n,0}}{\Delta t} = \frac{a_x}{\Delta x} f_{0i+1/2}^{*,1} - \frac{2a_x}{\Delta x} f_{0i}^{n,1} + \frac{a_x}{\Delta x} f_{0i-1/2}^{*,1}. \tag{2.34}$$

Inserting expressions (2.32) into (2.34) leads to equation (2.28) which is consistent with the limit diffusion equation (2.6). To complete the proof, it is necessary to show that f_1^{n+1} tends to zero as ε tends to zero. By using the diffusion scaling equation (2.10) rewrites under the form

$$f_{1i}^{n+1} = \frac{\varepsilon^2\zeta^3}{\varepsilon^2\zeta^3 + 2\sigma_i\Delta t}\left[f_{1i}^n - \frac{\Delta t}{\varepsilon}\left(\zeta\frac{f_{2i+1}^n - f_{2i-1}^n}{2\Delta x} - a_x\frac{f_{1i+1}^n - 2f_{1i}^n + f_{1i-1}^n}{2\Delta x}\right)\right]. \tag{2.35}$$

One directly observes that f_1^{n+1} tends to zero as ε tends to zero. □

The asymptotic-preserving property requires that the scheme should be uniformly stable with respect to the small parameter ε. In the case of an uniform stable scheme the CFL stability condition in diffusive regime should be that of a diffusion scheme $\Delta t \leq 3\alpha_{ei}\Delta x^2/\zeta^5$ (see Eq.2.7). Also, in the case of a small collisional parameter α_{ei}, the time step should be chosen according to the hyperbolic CFL condition $\Delta t \leq \Delta x/a_x$. An uniform stability property is proved in[56] or [62] in the framework of linear scalar equations. However, the model considered in this work is a nonlinear system and the derivation of such a property is very challenging. Therefore, for the numerical test cases we consider the following CFL condition

$$\Delta t \leq \max(\Delta x/a_x, 3\alpha_{ei}\Delta x^2/\zeta^5). \tag{2.36}$$

3. Homogeneous case with electric field

The second simplified model studied, is given by (1.1) without space dependency but considering an electric field. In this section, the difficulties encountered when using a relaxation-type method to include the source term $-\frac{E}{\zeta}(f_0 - f_2)$ are highlighted. Following the same procedure as in the case without electric field, a numerical scheme is proposed and the source term $-\frac{E}{\zeta}(f_0 - f_2)$ is taken into account. The scheme presented, satisfies a well-balanced property and is asymptotic-preserving. The collision coefficient α_{ei} is a function of x and is then constant in the present case. However, the method proposed here, is able to handle the case where α_{ei} depends on ζ. Without spatial dependency, the model (1.1) simplifies into

$$\begin{cases} \partial_t f_0 + E\partial_\zeta f_1 = 0, \\ \partial_t f_1 + E\partial_\zeta f_2 - \dfrac{E}{\zeta}(f_0 - f_2) = -\dfrac{2\alpha_{ei} f_1}{\zeta^3}. \end{cases} \tag{3.1}$$

Using the Hilbert expansions (2.3) as in the previous case, the following diffusion equation is obtained

$$\partial_t f_0^0(t,\zeta) - E\partial_\zeta\left(\frac{E\zeta^3}{6\alpha_{ei}}\partial_\zeta f_0^0(t,\zeta) - \frac{E\zeta^2}{3\alpha_{ei}} f_0^0(t,\zeta)\right) = 0. \tag{3.2}$$

3.1. Limit of the relaxation approach

Using the ideas introduced in [6], one can think of deriving a relaxation scheme for system (3.1). Even if the approach is similar, the relaxation scheme involved would be significantly different from the one proposed in [6] since the source term $-\frac{E}{\zeta}(f_0 - f_2)$ should be added. To assess such an issue, we first consider the collisionless case

$$\begin{cases} \partial_t f_0 + E\partial_\zeta f_1 = 0, \\ \partial_t f_1 + E\partial_\zeta f_2 - \dfrac{E}{\zeta}(f_0 - f_2) = 0. \end{cases} \tag{3.3}$$

Setting $\partial_\zeta z(\zeta) = 1/\zeta$, we propose the following relaxation model

$$\begin{cases} \partial_t f_0 + E\partial_\zeta \phi - E(f_1 - \phi)z'(\zeta) = 0, \\ \partial_t \phi + E\partial_\zeta f_0 - 2Ef_0 z'(\zeta) = \mu(f_1 - \phi), \\ \partial_t f_1 + E\partial_\zeta \pi - E(f_0 - \pi)z'(\zeta) = 0, \\ \partial_t \pi + E\partial_\zeta f_1 - 2Ef_1 z'(\zeta) = \mu(f_2 - \pi), \\ \partial_t z = 0, \end{cases} \tag{3.4}$$

where ϕ and π are relaxation variables. In the case $\mu = 0$, the previous system is hyperbolic, the eigenvalues are $-E$, 0, E and are associated with linearly degenerate fields. Hence, the Riemann problem can be solved.

In order to be consistent with the notations [6], we introduce

$$w = {}^t(f_0, \phi, f_1, \pi, z), \qquad \mathcal{U} = {}^t(f_0, f_1), \qquad \mathcal{F}(\mathcal{U}) = {}^t\big(Ef_1, Ef_2(f_0, f_1)\big) \tag{3.5}$$

Lemma 3.1. *Let $w_{L,R}$ be equilibrium constant states with $\phi^{L,R} = f_1^{L,R}$ and $\pi^{L,R} = f_2^{L,R}$. Defining the initial condition of (3.4) by $w_0(x) = w_L$ if $x < 0$ and $w_0(x) = w_R$ if $x > 0$ for $\mu = 0$, the solution of (3.4) writes*

$$w(x,t) = \begin{cases} w^L & if \quad x/t < -E, \\ w^{L*} & if \quad -E < x/t < 0, \\ w^{R*} & if \quad 0 < x/t < E, \\ w^R & if \quad E < x/t, \end{cases} \tag{3.6}$$

with

$$f_0^{L*,R*} = \frac{3(\zeta^{L,R})^2}{4(2(\zeta^R)^6 + 2(\zeta^L)^6 + 5(\zeta^R)^3(\zeta^L)^3)}\Big((-f_2^R - 2f_1^R + 3f_0^R)(\zeta^R)^4 + (-f_2^L + 2f_1^L + 3f_0^L)(\zeta^L)^4 + (f_2^L + 4f_1^L + 3f_0^L)(\zeta^R)^3(\zeta^L) + (f_2^R - 4f_1^R + 3f_0^R)(\zeta^R)(\zeta^L)^3\Big),$$

$$f_1^{L*,R*} = \frac{3(\zeta^{L,R})^2}{4(2(\zeta^R)^6 + 2(\zeta^L)^6 + 5(\zeta^R)^3(\zeta^L)^3)}\Big((3f_2^R - 2f_1^R - f_0^R)(\zeta^R)^4 + (-3f_2^L - 2f_1^L + f_0^L)(\zeta^L)^4 + (-3f_2^L - 4f_1^L - f_0^L)(\zeta^R)^3(\zeta^L) + (3f_2^R - 4f_1^R + f_0^R)(\zeta^R)(\zeta^L)^3\Big),$$

$$\begin{aligned} &z^{L*,R*} = z^{L,R}, \\ &\phi^{L*} = f_0^L + f_1^L - f_0^{L*}, \qquad \phi^{R*} = -f_0^R + f_1^R + f_0^{R*}, \\ &\pi^{L*} = f_1^L + f_2^L - f_1^{L*}, \qquad \pi^{R*} = -f_1^R + f_2^R + f_1^{R*}, \end{aligned}$$

and $\mathcal{U}^{L*,R*} = {}^t(f_0^{L*,R*}, f_1^{L*,R*})$ satisfy the admissibility conditions (1.4).

The computation of the intermediate states $\mathcal{U}^{L*,R*}$ is straightforward using the Riemann invariants given in Table 1. A long but easy calculation, using the expressions gives the admissibility conditions (1.4).

The relaxation model (3.4) enables the computation of a numerical scheme [9, 20, 52] for the model (3.3). However, one notices the complexity of the intermediate states $\mathcal{U}^{L*,R*}$ and an extension including the collisional term $-2\alpha_{ei} f_1/\zeta^3$ is very challenging. Different relaxation models were tested in order to include the collisional source term, but, because of their complexity, they lead to configurations where a Riemann invariant is missing and the problem remains unclosed. In a recent work [31], the same issue is encountered and an additional relation is arbitrarily imposed. In the present situation, this strategy leads to particularly inconvenient solutions and the admissibility conditions are lost.

TABLE 1. Features of the Riemann problem.

Eigenvalue	Multiplicity	Riemann Invariants	Eigenvectors
E	2	$f_0+\phi,\quad f_1+\pi,\ z$	${}^t(0,0,1,1,0),\quad {}^t(1,1,0,0,0)$
$-E$	2	$-f_0+\phi,\quad -f_1+\pi,\ z$	${}^t(0,0,-1,1,0),\quad {}^t(-1,1,0,0,0)$
0	1	$\frac{f_1}{\zeta^2},\ \frac{f_0}{\zeta^2},\ \zeta(\pi-f_0/3),\ \zeta(\phi-f_1/3)$	${}^t(2f_0,f_1-\phi,2f_1,f_0-\pi,1)$

3.2. The numerical method

The numerical approach presented in the case with electric field is now considered. Contrarily to the relaxation-type procedure, this method enables to include the source term $-\frac{E}{\zeta}(f_0-f_2)$ naturally.

Integrating the second equation of (3.1) on $[-a_\zeta \Delta t, a_\zeta \Delta t]\times[0,\Delta t]$ and multiplying by $\frac{1}{2a_\zeta\Delta t}$ gives the following expression

$$f_1^* = \frac{2a_\zeta\zeta^3}{2a_\zeta\zeta^3+2\alpha_{ei}\Delta\zeta}\left[\frac{f_1^L+f_1^R}{2}-\frac{1}{2a_\zeta}(Ef_2^R-Ef_2^L)+\frac{\Delta\zeta}{2a_\zeta}S_{L,R}\right], \tag{3.7}$$

with

$$S_{L,R}=\frac{1}{2}\left[\frac{E}{\zeta_R}(f_0^R-f_2^R)+\frac{E}{\zeta_L}(f_0^L-f_2^L)\right].$$

The unknowns f_0^{L*}, f_0^{R*} and f_0^{n+1} are computed following the same approach as in the first part

$$f_{0i}^{n+1}=\frac{a_\zeta\Delta t}{\Delta\zeta}f_{0i-1/2}^{R*}+\left(1-\frac{2a_\zeta\Delta t}{\Delta\zeta}\right)f_{0i}^n+\frac{a_\zeta\Delta t}{\Delta\zeta}f_{0i+1/2}^{L*}, \tag{3.8}$$

where the unknowns f_0^{R*} and f_0^{L*} are given by

$$\begin{cases} f_0^{L*}=\tilde{f}_0-\Gamma\theta,\\ f_0^{R*}=\tilde{f}_0+\Gamma\theta,\end{cases} \tag{3.9}$$

with

$$\Gamma=\frac{1}{2}\left[f_0^R-f_0^L-\frac{\zeta}{a_\zeta}(f_1^L-2f_1^*+f_1^R)\right]$$

and

$$\tilde{f}_0=\frac{f_0^L+f_0^R}{2}-\frac{1}{2a_\zeta}\left[\zeta f_1^R-\zeta f_1^L\right].$$

Using, the same arguments as in the case without electric field, we set $a_\zeta=|E|$. The following scheme is considered to compute f_{1i}^{n+1} at each time step

$$f_{1i}^{n+1}=\frac{\zeta_i^3}{\zeta_i^3+2\alpha_{ei}\Delta t}\left[f_{1i}^n-\Delta t\left(E\frac{f_{2i+1}^n-f_{2i-1}^n}{2\Delta\zeta}-a_\zeta\frac{f_{1i+1}^n-2f_{1i}^n+f_{1i-1}^n}{2\Delta\zeta}+\frac{E}{\zeta_i}(f_{0i}^n-f_{2i}^n)\right)\right]. \tag{3.10}$$

3.3. Properties

In this part, we are interested in the equilibrium solution of system (3.1). In particular, it is shown that the scheme (3.8)−(3.10) preserves this solution. Then, the asymptotic-preserving feature of the scheme is exhibited.

A stationary solution of system (3.1) satisfies

$$\begin{cases} E\dfrac{\partial f_1}{\partial \zeta} = 0, \\ E\dfrac{\partial f_2}{\partial \zeta} - \dfrac{E}{\zeta}(f_0 - f_2) = -\dfrac{2\alpha_{ei} f_1}{\zeta^3}. \end{cases} \tag{3.11}$$

The first equation of (3.11) implies that f_1 is independent of ζ. Using the definitions of the angular moments (1.2) and the definition (1.3), it follows that $f_1 = 0$ and $f_2 = f_0/3$. Indeed the definitions (1.2) imply $f_1 = 0$ in $\zeta = 0$. The second equation of the previous system is solved and gives the equilibrium solution of the model (3.1)

$$\begin{cases} f_0 = K\zeta^2, \\ f_1 = 0, \end{cases} \tag{3.12}$$

where K is a scalar constant.

Theorem 3.2. *The numerical scheme given by (3.8)–(3.10) is well-balanced in the sense that the stationary states (3.12) are exactly preserved by the scheme.*

Proof. Using the stationary states (3.12) into the definition (3.7) leads to

$$f_1^* = \frac{2a_\zeta \zeta^3}{a_\zeta \zeta^3 + 2\alpha_{ei}\Delta\zeta}\left[-\frac{1}{3a_\zeta}(EK\zeta_R^2 - EK\zeta_L^2) + \frac{\Delta\zeta EK}{3a_\zeta}(\zeta_R + \zeta_L)\right].$$

Since $(\zeta_R^2 - \zeta_L^2) = (\zeta_R + \zeta_L)(\zeta_R - \zeta_L) = (\zeta_R + \zeta_L)\Delta\zeta$, the calculation of the previous equation gives

$$f_1^* = 0.$$

The same calculation considering (3.10) leads to

$$f_1^{n+1} = 0.$$

Using the definition (2.23) it follows that

$$\begin{cases} f_0^{R*} = \dfrac{1}{2}[f_{0L} - \theta f_{0L} + f_{0R} + \theta f_{0R}], \\ f_0^{L*} = \dfrac{1}{2}[f_{0R} - \theta f_{0R} + f_{0L} + \theta f_{0L}]. \end{cases} \tag{3.13}$$

The initial conditions (3.12) imply that $\theta = 1$ and inserting (3.13) into equation (3.8) give

$$f_{0i}^{n+1} = \frac{a\Delta t}{\Delta\zeta}K\zeta_i^2 + \left(1 - \frac{2a\Delta t}{\Delta\zeta}\right)K\zeta_i^2 + \frac{a\Delta t}{\Delta\zeta}K\zeta_i^2.$$

Finally, the previous equation simplifies to give

$$f_{0i}^{n+1} = K\zeta_i^2.$$

The stationary solution (3.12) is then preserved by the scheme. □

Using the ideas introduced in the first section, we obtain that the scheme (3.8)–(3.10) is consistent with the limit diffusion equation (3.2) in the diffusive limit.

Theorem 3.3. *When ε tends to zero, the unknown f_0^{n+1} given by the numerical scheme (3.8)–(3.10) satisfies the following discrete equation*

$$\frac{f_{0i}^{n+1,0}-f_{0i}^{n,0}}{\Delta t}-\frac{E}{\Delta\zeta}\left[\frac{\zeta_{i+1/2}^3}{6\sigma\Delta\zeta}\left[\left(Ef_{0i+1}^{n,0}-Ef_{0i}^{n,0}\right)\right]\right.$$
$$\left.-\frac{\zeta_{i-1/2}^3}{6\sigma\Delta\zeta}\left[(Ef_{0i}^{n,0}-Ef_{0i-1}^{n,0})\right]+\frac{\zeta_{i+1/2}^3 S_{i+1/2}^{n,0}}{2\sigma}-\frac{\zeta_{i-1/2}^3 S_{i-1/2}^{n,0}}{2\sigma}\right]=0,$$

with

$$S_{i+1/2}^{n,0}=\frac{E}{3}\left[\frac{f_{0i+1}^{n,0}}{\zeta_{i+1}}+\frac{f_{0i}^{n,0}}{\zeta_i}\right].$$

Proof. The proof is the same as in the case without electric field. □

Following the procedure considered in the inhomogeneous case without electric field, in practice the following stability CFL condition is used

$$\Delta t\leq\max\left(\Delta\zeta/a_\zeta,3\alpha_{ei}\Delta\zeta^2/E^2\zeta_{\max}^3\right). \tag{3.14}$$

4. Numerical examples

In this section we compare the asymptotic-preserving scheme to the standard HLL scheme [44] and to an explicit discretisation of the diffusion equation in different regimes. For all the numerical test cases the time step considered for the asymptotic-preserving scheme is taken as the maximum of the hyperbolic time step and the diffusion time step (see CFL condition Eq. (2.36)). The numerical scheme is able to work with the diffusion time step when it becomes larger than the hyperbolic time step.

4.1. Free transport without electric field

We first consider system (2.1), without collisions, to validate the numerical scheme proposed in (2.10)–(2.18)–(2.23)–(2.26) on a simple advection of an initial profile. The solution is compared with the exact solution. Consider the initial conditions

$$\begin{cases} f_0(x,0)=\sqrt{\dfrac{2}{\pi}}\exp\left(-\dfrac{(x+5)^2}{2}\right),\\ f_1(x,0)=\sqrt{\dfrac{2}{\pi}}\exp\left(-\dfrac{(x+5)^2}{2}\right),\end{cases}$$

with periodical boundary conditions. In this case we have fixed $\zeta=5$. In Figure 2, we compare the numerical solution obtained with the scheme (2.10)–(2.18)–(2.23)–(2.26) displayed in dashed blue with the exact solution in red at time $t=6$ using $\Delta x=4\times10^{-3}$. In Table 2 the results of a convergence study are given. The scheme is first order accurate.

4.2. Temperature gradient with collisions without electric field

We now consider the system equation (2.1) with collisions to validate the numerical scheme (2.10)–(2.18)–(2.23)–(2.26) taking into account the collisional part. The solution obtained with the scheme presented in this paper is compared with the classical HLL scheme.

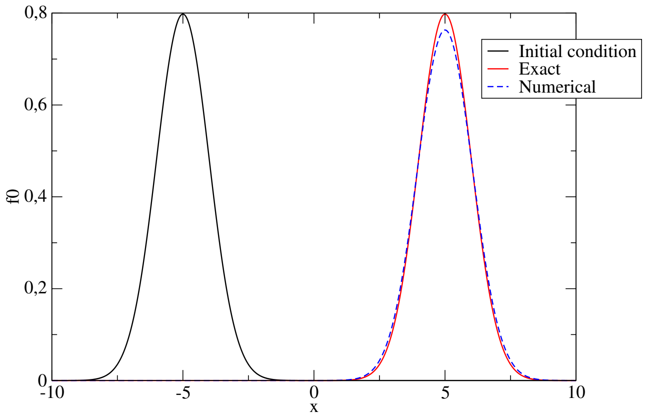

FIGURE 2. Free transport: comparison of the numerical solution for $\Delta x = 4 \times 10^{-3}$ and the exact solution (*red*) at time $t = 6$. (Color online)

TABLE 2. Convergence study of the method. The order of the method is given for the L^1, L^2 and L^∞ norms.

Δx	L^1 error	L^1 order	L^2 error	L^2 order	L^∞ error	L^∞ order
4×10^{-2}	0.63	–	0.27	–	0.22	–
2×10^{-2}	0.36	0.77	0.17	0.7	0.14	0.65
1×10^{-2}	0.20	0.88	0.09	0.83	0.08	0.84
6.66×10^{-3}	0.14	0.88	0.06	0.9	0.06	0.87
5×10^{-3}	0.11	0.84	0.05	0.92	0.04	0.91
4×10^{-3}	0.08	1.09	0.04	0.95	0.03	0.93

Consider the initial conditions

$$\begin{cases} f_0(x,\zeta,0) = \sqrt{\dfrac{2}{\pi}} \dfrac{\zeta^2}{T_{\text{ini}}(x)^{3/2}} \exp\left(-\dfrac{\zeta^2}{2T_{\text{ini}}(x)}\right), \\ f_1(x,\zeta,0) = 0, \end{cases}$$

with

$$T_{\text{ini}}(x) = 2 - \arctan(x)$$

and $\alpha_{ei} = 1$. On the right and left boundaries, we use a Neumann boundary condition: the values of f_0 and f_1 in the boundary ghost cells are set to the values in the corresponding real boundary cells. The energy range chosen is $[0, 12]$ with an energy step $\Delta\zeta = 0.1$ and the space range is $[-40, 40]$ with a space step $\Delta x = 0.2$. In Figure 3, we compare the numerical solution obtained with the AP scheme (2.18)–(2.23)–(2.26). The solution obtained with the Asymptotic-preserving scheme is displayed in continuous lines with the solution given by HLL scheme in dashed lines at time 0.25 and 0.5. The Asymptotic-preserving numerical scheme and the HLL scheme gives comparable results.

4.3. Temperature gradient in the diffusive regime without electric field

In this numerical test, the same initial and boundary conditions that in the test case 3.2 are chosen. However, we consider a large collisional parameter and take $\alpha_{ei} = 10^4$. The scheme (3.8)–(3.10) is studied in the diffusive regime. The results are compared with the diffusion solution and with the ones obtained with the HLL scheme. In Figure 4 the results obtained with the asymptotic-preserving scheme are displayed in continuous green lines

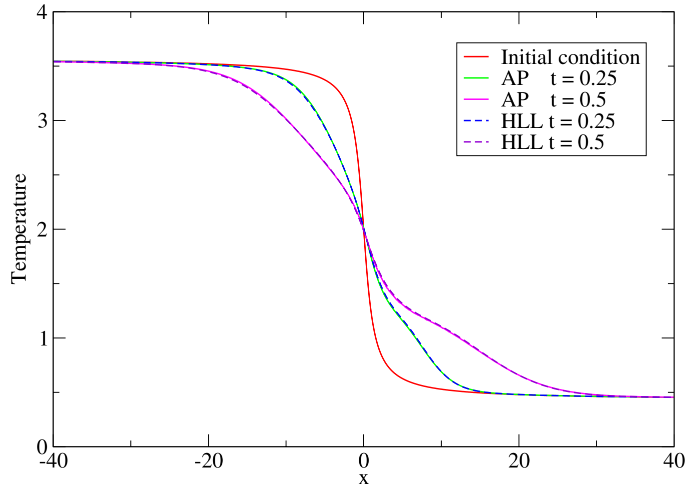

FIGURE 3. Temperature gradient: comparison of the temperature profile for the numerical solution (AP) and for the HLL scheme (HLL) at time 0.25 and 0.5.

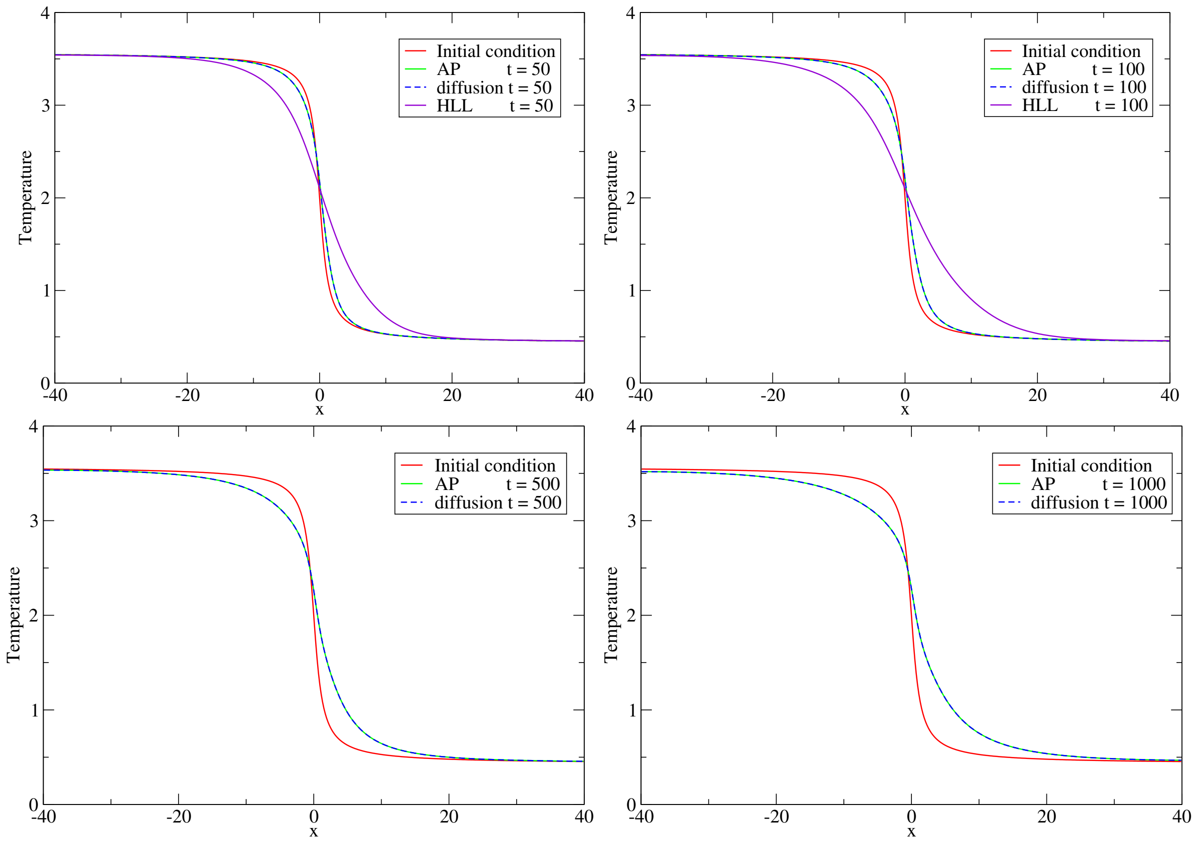

FIGURE 4. Temperature gradient in the diffusive limit: comparison of the temperature profile of the asymptotic-preserving scheme (AP), the HLL scheme (HLL) and the diffusion solution at time $t = 50$, 100, 500 and 1000.

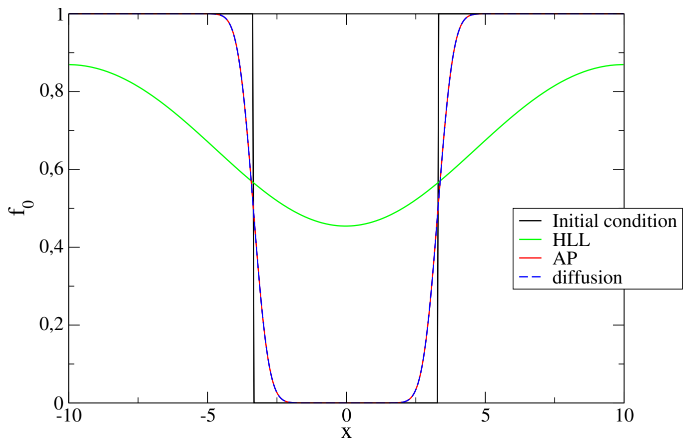

FIGURE 5. Comparison of the f_0 profile for the asymptotic-preserving scheme (AP), for the HLL scheme (HLL) and the diffusion solution at time $t = 200$.

with the solution given by HLL scheme in continuous purple lines and the diffusion solution in dashed blue lines at time $t = 50$, $t = 100$, 500 and 1000. The AP numerical scheme and the diffusion solution match perfectly while we remark for time $t = 50$ and $t = 100$ that the HLL scheme gives very inaccurate results. The results obtained with the HLL scheme at time $t = 500$ and $t = 1000$ are completely wrong and are not displayed, however we notice that in the long time regime the AP numerical scheme and the diffusion solution still match.

4.4. Discontinuous initial condition in the diffusive regime without electric field

In this case, a discontinuous initial condition in the diffusive regime without electric field is considered. The results are compared with the diffusion equation solution and the HLL scheme. The energy range chosen is $[0, 6]$ with an energy step $\Delta\zeta = 0.1$ and the space range L=$[-10, 10]$ with a space step $\Delta x = 5 \times 10^{-2}$. Consider the initial conditions

$$\begin{cases} f_0(x,\zeta,0) = \begin{cases} 1 & \text{if} \quad x \leq L/3, \\ 0 & \text{if} \quad L/3 \leq x \leq 2L/3, \\ 1 & \text{if} \quad L/3 \leq x, \end{cases} \\ f_1(x,\zeta,0) = 0, \end{cases}$$

with periodical boundary conditions and $\alpha_{ei} = 10^4$. In Figure 5, we compare the numerical solution obtained with the Asymptotic-preserving scheme displayed in red with the diffusion solution in dashed blue and the HLL scheme in green at time $t = 200$. The AP and diffusion solutions match perfectly while the HLL scheme is very inaccurate. In Figure 6, the long time behaviour of the numerical solutions is considered. The AP scheme and the diffusion solution are compared at time $t = 500$, the results match.

4.5. Relaxation of a Gaussian profile, in the homogeneous case in the diffusive regime with electric field

We consider system (3.1) with collisions and the source term $\frac{E}{\zeta}(f_0 - f_2)$ to validate the numerical scheme (3.8)–(3.10) in the diffusive limit. On the left and right boundaries, we use Neumann boundary conditions: the values of f_0 and f_1 in the boundary ghost cells are set to the values in the corresponding real boundary cells. Here $\alpha_{ei} = 10^4$ and the energy range chosen is $[0, 20]$ with an energy step $\Delta\zeta = 10^{-2}$.

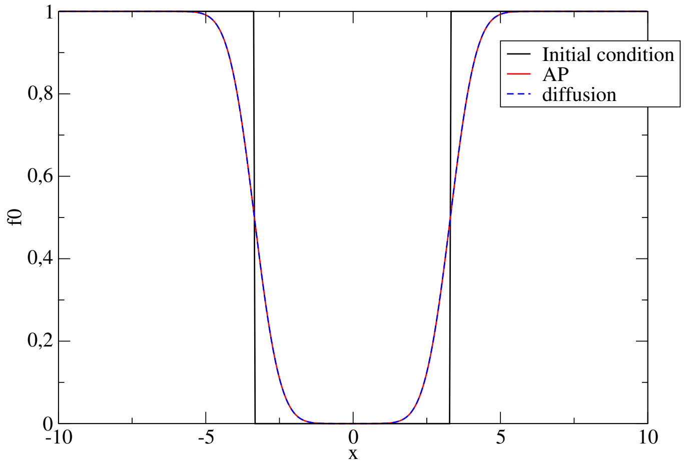

FIGURE 6. Comparison of the f_0 profile for the Asymptotic-preserving scheme (AP), and the diffusion solution at time $t = 500$.

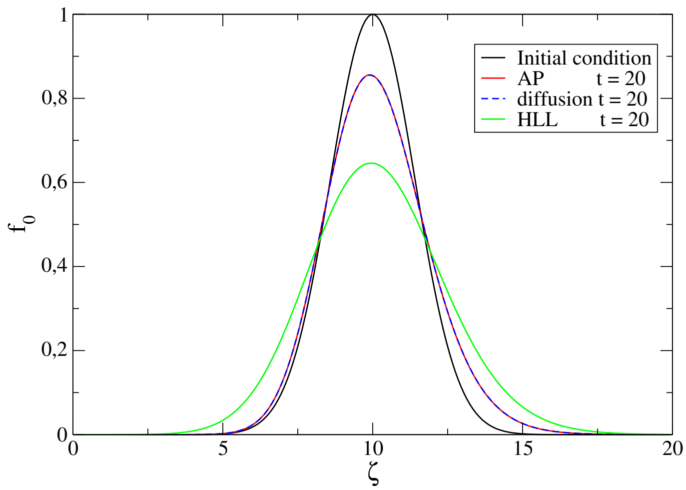

FIGURE 7. Relaxation of a Gaussian profile: comparison of the f_0 profile for the asymptotic-preserving scheme (AP), for the HLL scheme (HLL) and the diffusion solution at time $t = 20$.

Here we have chosen $E = 1$ and considered the following initial conditions

$$\begin{cases} f_0(\zeta, 0) = \sqrt{\dfrac{2}{\pi}} \exp\left(-\dfrac{\zeta^2}{2}\right), \\ f_1(\zeta, 0) = 0. \end{cases}$$

In Figure 7, we compare the numerical solution obtained with the scheme (3.8)−(3.10) displayed in red with the diffusion solution in dashed blue and the HLL scheme at time $t = 20$. The asymptotic-preserving and diffusion solutions match perfectly while the HLL scheme is very diffusive. In Figure 8, the results obtained with the AP scheme and the diffusion solution are compared in the long time regime at time $t = 80$.

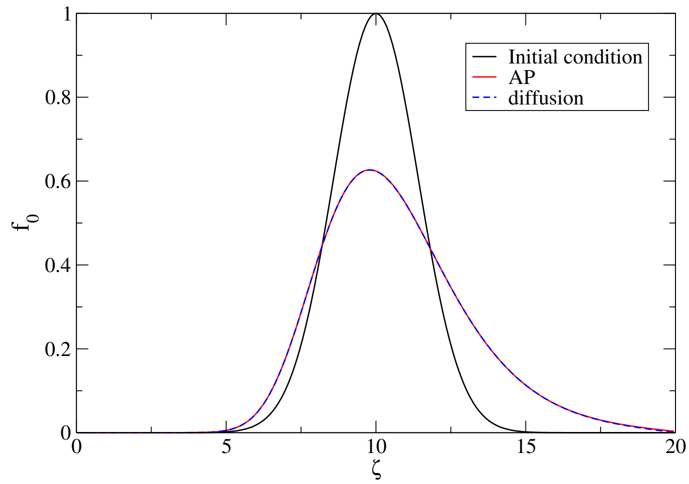

FIGURE 8. Relaxation of a Gaussian profile: comparison of the f_0 profile for the asymptotic-preserving scheme (AP) and the diffusion solution at time $t = 80$.

4.6. Relaxation of a Gaussian profile in the diffusive regime without electric field in the case of a non-constant collisional parameter

In this example, the numerical scheme (2.10)−(2.18)−(2.23)−(2.26) is verified in the diffusive regime without electric field in a inhomogeneous collisional plasma. In this case the coefficient α_{ei} is not constant and follows the linear profile

$$\alpha_{ei}(x) = (5x/8 + 15/2) \times 10^3.$$

Then $\alpha_{ei}(-4) = 5 \times 10^3$ and $\alpha_{ei}(4) = 10^4$. On the left and right boundaries, we use Neumann boundary conditions: the values of f_0 and f_1 in the boundary ghost cells are set to the values in the corresponding real boundary cells. The energy range chosen is $[0, 8]$ with an energy step $\Delta\zeta = 0.1$ and the space range $[-4, 4]$ with a space step $\Delta x = 5 \times 10^{-2}$. The initial conditions are the following

$$\begin{cases} f_0(x, \zeta, 0) = \zeta^2 \exp\left(-\dfrac{x^2}{2}\right), \\ f_1(x, \zeta, 0) = 0. \end{cases}$$

In Figure 9, we compare the numerical solution obtained with the asymptotic-preserving scheme displayed in red with the diffusion solution in dashed blue at time $t = 150$. In this case, the asymptotic-preserving and diffusion solutions also match perfectly. The HLL scheme results are not given in Figure 9, since the final time $t = 150$ is important the HLL results are completely wrong.

5. CONCLUSION

In this work, we have proposed a numerical scheme for the electronic M_1 model in the case without electric field and in the homogeneous case. We have exhibited an approximate Riemann solver that satisfies the admissibility conditions. Contrarily to the HLL scheme, the proposed numerical scheme is asymptotic-preserving and recovers the correct diffusion equation in the diffusive limit. It has been shown, in the homogeneous case, that the method presented, enables to include the source term $-E(f_0 - f_2)/\zeta$, while a relaxation type method seems inconvenient. In addition, the scheme is well-balanced, capturing the steady state considered. Several numerical tests have been performed, it has been shown that the presented scheme behaves correctly in the classical

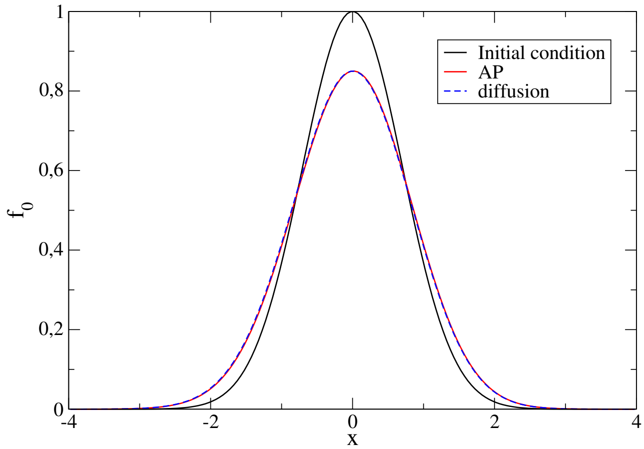

FIGURE 9. Relaxation of a Gaussian profile in the case of a linear collisional parameter: comparison of the f_0 profile for the asymptotic-preserving scheme (AP) and the diffusion solution at time $t = 150$.

regime and in the diffusive limit. Indeed, while, the HLL scheme is very inaccurate in the diffusive regime, the asymptotic-preserving scheme matches perfectly with the expected diffusion solution. Also, the method correctly handles the case where the collisional parameter is not constant. The present study can be extended to the general electronic M_1 model (1.1). However, the correct treatment of the mixed-derivatives, arising in the diffusive limit when considering the entire model is a challenging issue. This problem will be investigated in a forthcoming separate study.

REFERENCES

[1] A. Bermudez and M.E. Vazquez, Upwind methods for hyperbolic conservation laws with source terms. *Comput. Fluids* **23** (1994) 1049–1071.

[2] G.W. Alldredge, C.D. Hauck and A.L. Tits, High-order entropy-based closures for linear transport in slab geometry II: A computational study of the optimization problem. *SIAM J. Sci. Comput.* **34** (2012) B361–B391.

[3] E. Audit, P. Charrier, J.-P. Chièze and B. Dubroca, A radiation hydrodynamics scheme valid from the transport to the diffusion limit. Preprint arXiv:astro-ph/0206281 (2002).

[4] R. Balescu. Transport Processes in Plasma, Vol. 1. Elsevier, Amsterdam (1988).

[5] M. Bennoune, M. Lemou and L. Mieussens, Uniformly stable numerical schemes for the Boltzmann equation preserving the compressible Navier Stokes asymptotics. *J. Comput. Phys.* **227** (2008) 3781–3803.

[6] C. Berthon, P. Charrier and B. Dubroca, An asymptotic preserving relaxation scheme for a moment model of radiative transfer. *C.R. Acad. Sci. Paris, Ser. I* **344** (2007) 467–472.

[7] C. Berthon, P. Charrier and B. Dubroca, An HLLC Scheme to Solve The M1 Model of Radiative Transfer in Two Space Dimensions. *J. Scient. Comput.* **31** (2007) 347–389.

[8] C. Berthon and R. Turpault, Asymptotic preserving HLL schemes. *Numer. Methods Partial Differ. Equ.* **27** (2011) 1396–1422.

[9] F. Bouchut, Nonlinear Stability of Finite Volume Methods for Hyperbolic Conservation Laws, and Well-Balanced Schemes for sources. *Frontiers in Mathematics series*. Birkhauser (2004).

[10] F. Bouchut and T. Morales, A subsonic-well-balanced reconstruction scheme for shallow water flows. *SIAM J. Numer. Anal.* **48** (2010) 1733–1758.

[11] S.I. Braginskii, Reviews of Plasma Physics. In vol. 1. Edited by M.A Leontovich. Consultants Bureau New York (1965) 205.

[12] A.V. Brantov, V.Yu. Bychenkov, O.V. Batishchev and W. Rozmus, Nonlocal heat wave propagation due to skin layer plasma heating by short laser pulses. *Comput. Phys. Commun.* **164** (2004) 67.

[13] C. Buet and S. Cordier, Asymptotic Preserving Scheme and Numerical Methods for Radiative Hydrodynamic Models. *C.R. Acad. Sci. Paris, Tome, Série I* **338** (2004) 951–956.

[14] C. Buet, S. Cordier, B. Lucquin-Desreux and S. Mancini, Diffusion limit of the Lorentz model: asymptotic preserving schemes. *ESAIM: M2AN* **36** (2002) 631–655.

[15] C. Buet and B. Després, Asymptotic analysis of fluid models for the coupling of radiation and hydrodynamics. *J. Quant. Spectrosc. Radiat. Transfer* **85** (2004) 385–418.

[16] C. Buet and B. Després, Asymptotic preserving and positive schemes for radiation hydrodynamics. *J. Comptut. Phys.* **215** (2006) 717–740.

[17] R. Caflish, S. Jin and G. Russo, Uniformly accurate schemes for hyperbolic systems with relaxation. *SIAM J. Numer. Anal.* **34** (1997) 246–281.

[18] P. Cargo and A.-Y. Le Roux, Un schéma équilibre adapté au modèle d'atmosphère avec termes de gravité. *C.R. Acad. Sci. , Ser. I* **318** (1994) 73–76.

[19] J.A. Carrillo, T. Goudon, P. Lafitte and F. Vecil, Numerical schemes of diffusion asymptotics and moment closures for kinetic equations. *J. Sci. Comput.* **36** (2008) 113–149.

[20] C.Berthon, Numerical approximations of the 10-moment Gaussian closure. *Math. Comput.* **75** (2006) 1809–1831.

[21] C. Chalons, F. Coquel, E. Godlewski, P.-A. Raviart and N. Seguin, Godunov-type schemes for hyperbolic systems with parameter-dependent source. The case of Euler system with friction. *Math. Models Methods Appl. Sci.* **20** (2010) 2109–2166. MR 2740716 (2011m:65179).

[22] C. Chalons, F. Coquel and C. Marmignon, Well-balanced time implicit formulation of relaxation schemes for the euler equations. *SIAM J. Sci. Comput.* **30** (2008) 394–415.

[23] S. Chapman and T.G. Cowling, The Mathematical Theory of Non-Uniform Gases. Cambridge University Press, Cambridge, England (1995).

[24] P. Charrier, B. Dubroca, G. Duffa and R. Turpault, Multigroup model for radiating flows during atmospheric hypersonic re-entry. Proceedings of International Workshop on Radiation of High Temperature Gases in Atmospheric Entry. Lisbonne, Portugal (2003) 103–110.

[25] F. Coron and B. Perthame, Numerical passage from kinetic to fluid equations. *SIAM J. Numer. Anal.* **28** (1991) 26–42.

[26] P. Crispel, P. Degond and M.-H. Vignal, Quasi-neutral fluid models for current-carrying plasmas. *J. Comput. Phys.* **205** (2005) 408–438.

[27] P. Crispel, P. Degond and M.-H. Vignal, An asymptotic preserving scheme for the two-fluid Euler-Poisson model in the quasi-neutral limit. *J. Comput. Phys.* **223** (2007) 208–234.

[28] P. Degond, F. Deluzet, L. Navoret, A. Sun and M. Vignal, Asymptotic-Preserving Particle-In-Cell method for the Vlasov-Poisson system near quasineutrality. *J. Comput. Phys.* **229** (2010) 5630–5652.

[29] P. Degond, H. Liu, D. Savelief and M-H. Vignal, Numerical approximation of the Euler-Poisson-Boltzmann model in the quasineutral limit. *C.R. Acad. Sci. Paris, Ser. I* **341** (2005) 323–328.

[30] P. Degond, D. Savelief and F. Deluzet, Numerical approximation of the Euler-Maxwell model in the quasineutral limit. *J. Comput. Phys.* **231** (2012) 1917–1946.

[31] V. Desveaux, M. Zenk, C. Berthon and C. Klingenberg, Well-balanced schemes to capture non-explicit steady states. Part 1: Ripa model. *Math. Comput.* **85** (2016) 1571–1602.

[32] J.F. Drake, P.K. Kaw, Y.C. Lee, G. Schmidt, C.S. Liu and M.N. Rosenbluth, Parametric instabilities of electromagnetic waves in plasmas. *Phys. Fluids* **17** (1974) 778.

[33] B. Dubroca, J.-L. Feugeas and M. Frank, Angular moment model for the Fokker-Planck equation. *Europ. Phys. J. D* **60** (2010) 301.

[34] B. Dubroca and J.L. Feugeas, étude théorique et numérique d'une hiéarchie de modèles aux moments pour le transfert radiatif. *C.R. Acad. Sci. Paris, Ser. I* **329** (1999) 915–920.

[35] B. Dubroca and J.L. Feugeas, Entropic moment closure hierarchy for the radiative transfert equation. *C.R. Acad. Sci. Paris Ser. I* **329** (1999) 915.

[36] E. Epperlein and R. Short, *Phys. Fluids* B **4** (1992) 2211.

[37] G. Gallice, Positive and entropy stable Godunov-type schemes for gas dynamics and MHD equations in Lagrangian or Eulerian coordinates. *Numer. Math.* **94** (2003) 673–713. MR 1990589 (2004e:65094).

[38] L. Gosse and G. Toscani, An asymptotic-preserving well-balanced scheme for the hyperbolic heat equations. *C.R. Math. Acad. Sci. Paris* **334** (2002) 337–342.

[39] L. Gosse and G. Toscani, Space localization and well-balanced schemes for discrete kinetic models in diffusive regimes. *SIAM J. Numer. Anal.* **41** (2003) 641–658.

[40] H. Grad. On the kinetic theory of rarefied gases. *Commun. Pure Appl. Math.* **2** (1949) 331–407.

[41] J. M. Greenberg and A.Y. Leroux, A well-balanced scheme for the numerical processing of source terms in hyperbolic equations. *SIAM J. Numer. Anal.* **33** (1996) 1–16.

[42] C.P.T. Groth and J.G. McDonald, Towards physically-realizable and hyperbolic moment closures for kinetic theory. *Continuum Mech. Thermodyn.* **21** (2009) 467–493.

[43] S. Guisset, S. Brull, B. Dubroca, E. d'Humières, S. Karpov and I. Potapenko, Asymptotic-preserving scheme for the Fokker-Planck-Landau-Maxwell system in the quasi-neutral regime. *Commun. Comput. Phys.* **19** (2016) 301–328.

[44] A. Harten, P.D. Lax and B. Van Leer, On upstream differencing and Godunov-type schemes for hyperbolic conservation laws. *SIAM Rev.* **25** (1983) 35–61.

[45] P. Lafitte J.A. Carrillo and T. Goudon, Simulation of fluid and particles flows: asymptotic preserving schemes for bubbling and flowing regimes. *J. Comput. Phys.* **227** (2008) 7929–7951.

[46] S. Jin, Efficient Asymptotic-Preserving (AP) Schemes for Some Multiscale Kinetic Equations. *SIAM J. Sci. Comput.* **21** (1999) 441–454.

[47] S. Jin and C.D. Levermore, Fully discrete numerical transfer in diffusive regimes. *Trans. Theory Stat. Phys.* **22** (1993) 739–9791.

[48] S. Jin and C.D. Levermore, The discrete-ordinate method in diffusive regimes. *Trans. Theory Stat. Phys.* **20** (1991) 413–439.

[49] S. Jin and D. Levermore, Numerical Schemes for Hyperbolic Conservation Laws with Stiff Relaxation Terms. *J. Comput. Phys.* **126** (1996) 449-467.

[50] S. Jin and L. Pareschi, Discretization of the multiscale semiconductor Boltzmann equation by diffusive relaxation scheme. *J. Comput. Phys.* **161** (2000) 312–330.

[51] S. Jin, L. Pareschi and G. Toscani, Uniformly accurate diffusive relaxation schemes for multiscale transport equations. *SIAM J. Numer. Anal.* **38** (2000) 913–936.

[52] S. Jin and Z. Xin, The relaxation scheme for systems of conservation laws in arbitrary space dimension. *Commun. Pure Appl. Math.* **45** (1995) 235–276.

[53] A. Klar, An asymptotic-induced scheme for nonstationary transport equations in the diffusive limit. *SIAM J. Numer. Anal.* **35** (1998) 1073–1094.

[54] A. Klar, An asymptotic preserving numerical scheme for kinetic equations in the low Mach number limit. *SIAM J. Numer. Anal.* **36** (1999) 1507–1527.

[55] A. Klar and C. Schmeiser, Numerical passage from radiative heat transfer to nonlinear diffusion models. *Math. Models Methods Appl. Sci.* **11** (2001) 749–767.

[56] A. Klar and A. Unterreiter, Uniform stability of a finite difference scheme for transport equations in the diffusion limit. *SIAM J. Numer. Anal.* **40** (2002) 891–913.

[57] L. Landau, On the vibration of the electronic plasma. *J. Phys. (USSR)* **10** (1946) 25–34.

[58] A.W. Larsen and J.E. Morel, Asymptotic solutions of numerical transport problems in optically thick, diffusive regimes II. *J. Comput. Phys.* **83** (1989) 212–236.

[59] A.W. Larsen, J.E. Morel and W.F. Miller Jr, Asymptotic solutions of numerical transport problems in optically thick, diffusive regimes. *J. Comput. Phys.* **69** (1987) 283–324.

[60] M. Lemou and L. Mieussens, A new asymptotic preserving scheme based on micro-macro formulation for linear kinetic equations in the diffusion limit. *SIAM J. Sci. Comput.* **31** (2008) 334–368.

[61] C.D. Levermore, Moment closure hierarchies for kinetic theories. *J. Stat. Phys.* **83** (1996) 1021–1065.

[62] J. Liu and L. Mieussens, Analysis of an asymptotic preserving scheme for linear kinetic equations in the diffusion limit. *SIAM J. Numer. Anal.* **48** (2010) 7561–7586.

[63] J. Mallet, S. Brull and B. Dubroca, An entropic scheme for an angular moment model for the classical Fokker-Planck-Landeau equation of electrons. *Commun. Comput. Phys.* **15** (2015) 422–450.

[64] J. Mallet, S. Brull and B. Dubroca, General moment system for plasma physics based on minimum entropy principle. *Kinetic Relat Mod.* **8** (2015) 533–558.

[65] A. Marocchino, M. Tzoufras, S. Atzeni, A. Schiavi, Ph. D. Nicolaï, J. Mallet, V. Tikhonchuk and J.-L. Feugeas, Nonlocal heat wave propagation due to skin layer plasma heating by short laser pulses. *Phys. Plasmas* **20** (2013) 022702.

[66] J.G. McDonald and C.P.T. Groth, Towards realizable hyperbolic moment closures for viscous heat-conducting gas flows based on a maximum-entropy distribution. *Contin. Mech. Thermodyn.* **25** (2012) 573–603.

[67] N. Meezan, L. Divol, M. Marinak, G. Kerbel, L. Suter, R. Stevenson, G. Slark and K. Oades, *Phys. Plasmas* **11** (2004) 5573.

[68] G.N. Minerbo, Maximum entropy Eddigton Factors. *J. Quant. Spectrosc. Radiat. Transfer* **20** (1978) 541.

[69] I. Muller and T. Ruggeri, Rational Extended Thermodynamics. Springer, New York (1998).

[70] Ph. Nicolaï, M. Vandenboomgaerde, B. Canaud and F. Chaigneau. *Phys. Plasmas* **7** (2000) 4250.

[71] J.-F. Ripoll. An averaged formulation of the M1 radiation model with presumed probability density function for turbulent flows. *J. Quant. Spectrosc. Radiat. Trans.* **83** (2004) 493–517.

[72] J.-F. Ripoll, B. Dubroca and E. Audit, A factored operator method for solving coupled radiation-hydrodynamics models. *Trans. Theory. Stat. Phys.* **31** (2002) 531–557.

[73] W. Rozmus, V.T. Tikhonchuk and R. Cauble, A model of ultrashort laser pulse absorption in solid targets. *Phys. Plasmas* **3** (1996) 360.

[74] K. Shigemori, H. Azechi, M. Nakai, M. Honda, K. Meguro, N. Miyanaga, H. Takabe and K. Mima, *Phys. Rev. Lett.* **78** (1997) 250.

[75] I.P. Shkarofsky and T.W. Johnston, and The Particle Kinetics of Plasmas M.P. Bachynski, Addison-Wesley Reading, Massachusetts (1966).

[76] L. Spitzer and R. Härm, *Phys. Rev.* **89** (1953) 977.

[77] H. Struchtrup, Macroscopic Transport Equations for Rarefied Gas Flows. Springer, Berlin (2005).

[78] E.F. Toro, Riemann Solvers and Numerical Methods for Fluids dynamics. Springer, Berlin (1999).

[79] R. Turpault, A consistent multigroup model for radiative transfer and its underlying mean opacity. *J. Quant. Spectrosc. Radiat. Transfer* **94** (2005) 357–371.

[80] R. Turpault, M. Frank, B. Dubroca and A. Klar, Multigroup half space moment appproximations to the radiative heat transfer equations. *J. Comput. Phys.* **198** (2004) 363.

[81] A. Velikovich, J. Dahlburg, J. Gardner and R. Taylor, *Phys. Plasmas* **5** (1998) 1491.